Journal of Hepatocellular Carcinoma

Dovepress
Taylor & Francis Group

Open Access Full Text Article

ORIGINAL RESEARCH

Prognostic Signature of NETs-Related Genes in Hepatocellular Carcinoma Based on Bulk and Single-Cell Transcriptomics

Ningning Lu[1,*], Zhixia Gu[2–5,*], Xiaoxue Yuan[2–5], Ronghua Jin[2–5], Jianjun Li[1]

[1]Interventional Therapy Center for Oncology, Beijing You'an Hospital, Capital Medical University, Beijing, 100015, People's Republic of China; [2]National Key Laboratory of Intelligent Tracking and Forecasting for Infectious Diseases, Beijing Ditan Hospital, Capital Medical University, Beijing, 100015, People's Republic of China; [3]Beijing Institute of Infectious Diseases, Beijing, 100015, People's Republic of China; [4]National Center for Infectious Diseases, Beijing Ditan Hospital, Capital Medical University, Beijing, 100015, People's Republic of China; [5]Beijing Key Laboratory of Emerging Infectious Diseases, Institute of Infectious Diseases, Beijing Ditan Hospital, Capital Medical University, Beijing, 100015, People's Republic of China

*These authors contributed equally to this work

Correspondence: Ronghua Jin; Jianjun Li, Email ronghuajin@ccmu.edu.cn; ljjir@ccmu.edu.cn

Background: Inflammation drives tumor development, with neutrophil extracellular traps (NETs) promoting progression through metastasis, immune suppression, and microenvironment modulation. However, the role of NETs-related genes in hepatocellular carcinoma (HCC) immunity response is still unclear.

Methods: We integrated single-cell RNA sequencing (GSE202642, seven tumor samples and four normal liver samples) and The Cancer Genome Atlas (TCGA, n=312) transcriptomic data to identify NETs-related gene signatures. Weighted gene co-expression network analysis (WGCNA) identified NETs-correlated gene modules, and LASSO-COX regression selected prognostic genes for risk stratification. A nomogram was developed to predict survival, while functional, mutation, immune, and drug sensitivity analyses highlighted intergroup differences. EdU and CCK-8 cell proliferation assays confirmed the role of NETs-related genes in HCC cell proliferation.

Results: The analysis revealed significant differences in survival time between high- and low-NETs groups. GAS2L3 and RTN3 were identified and validated as independent prognostic factors. ROC and decision curve analysis (DCA) demonstrated that the nomogram model combining NETs risk scores with clinical parameters exhibited robust prognostic performance. The high-risk subgroup was enriched in glycosphingolipid biosynthesis pathways and showed higher mutati843on rates, especially in TP53, CTNNB1, and MUC16, along with overexpression of immunosuppressive genes (VTCN1, LAIR1). In vitro experiments confirmed that GAS2L3 knockdown inhibited HepG2 and Huh7 cell proliferation.

Conclusion: Integrated multi-omics analysis revealed NETs-associated prognostic signatures in HCC, with GAS2L3 identified as a key gene linking NETs to tumor progression and therapeutic potential.

Keywords: hepatocellular carcinoma, single-cell RNA sequencing, NETs-related genes, GAS2L3, immune infiltration, prognostic model

Introduction

Hepatocellular carcinoma (HCC) is a prevalent global health threat with high malignancy and poor survival outcomes.[1,2] Despite the remarkable progress achieved in deciphering the intricate molecular mechanisms underpinning HCC development and progression, its clinical management remains a complex and arduous task. Current therapeutic strategies encompass surgical resection, liver transplantation, local ablation, transcatheter arterial chemoembolization (TACE), targeted therapy, and immunotherapy.[2] Notably, over 50% of advanced HCC patients require systemic treatment, yet only 30% demonstrate durable responses to existing immunotherapies, with median overall survival (OS) remaining below two years.[3,4] Recent studies have highlighted the importance of the tumor microenvironment (TME) in HCC progression, particularly the dynamic crosstalk between neoplastic cells, stromal components, and immune

Received: 11 June 2025
Accepted: 26 September 2025
Published: 15 October 2025

infiltrates.[5,6] This biological complexity necessitates the development of TME based prognostic biomarkers and personalized therapeutic strategies to improve clinical outcomes.

Driven by advances in high-throughput sequencing, large-scale international initiatives—including The Cancer Genome Atlas (TCGA), The International Cancer Genome Consortium (ICGC), and The Cancer Cell Line Encyclopedia (CCLE)—have generated comprehensive multi-omics datasets from matched patient cohorts. Analysis of these rich data resources has enabled the identification of genes critically involved in tumor initiation and progression, known as driver genes,[7] which include both oncogenes and tumor suppressor genes. Studies have shown that dysregulated Runt-related (RUNX) family genes (RUNX1, RUNX2, and RUNX3) may be involved in hepatocarcinogenesis from the earliest to the latest stages.[8] Nearly half of HCC patients harbor at least one recurrent oncogenic mutation, such as in TP53, CTNNB1, or TERT, which contribute to the establishment of an immunosuppressive microenvironment by modulating immune cell functions.[9]

Inflammation is closely associated with tumor development, and inflammatory cells and cytokines actively contribute to the inflammatory TME. Neutrophils, accounting for 50–70% of all circulating white blood cells, are crucial for tumor immune immunity.[10,11] Tumor-associated neutrophils (TAN), a subset of neutrophils that infiltrate tumors, correlate with aggressive phenotypes and poor prognosis.[12] Neutrophil extracellular traps (NETs) represent an inflammatory cell death mechanism in which neutrophils release a reticular DNA structure encapsulated by histones, proteases, and antimicrobial proteins to capture microorganisms and pathogens.[13–15] Studies have shown that modulating NETs in different ways can improve the outcomes of many diseases and increase survival rates.[16] NETs regulate the balance between Th1 and Th2 $CD4^+$ T cells and impair the anti-tumor function of NK cells.[12,17] Moreover, NETs are also closely related to tumor growth, development, and metastasis.[18–21] It can promote tumor cell migration by producing neutrophil elastase (NE). NETs contribute to tumor progression by promoting fibrin formation, facilitating thrombosis, and inducing T-cell exhaustion, which collectively enhances metastatic potential and suppresses anti-tumor immunity.[13,22–24] Prognostic signatures based on NETs-related genes have been reported in colorectal cancer,[25] breast cancer,[26] and lung adenocarcinoma,[27] and have been shown to help assess prognosis and response to chemotherapy or immunotherapy in cancer patients.

Despite these advances, the functional roles of NETosis-related genes in HCC immune regulation and therapeutic response remain incompletely understood, largely owing to studies that either depend solely on single datasets (such as TCGA) or lack in vitro experimental validation.[28,29] In this study, we integrated single-cell RNA sequencing data with TCGA resources to identify key NETs-related genes associated with HCC prognosis using advanced machine learning techniques. We developed a robust predictive model and performed comprehensive validation to ensure its prognostic relevance, offering novel insights into precision medicine strategies for HCC management. These results may provide a framework for advancing individualized treatment approaches in HCC.

Methods

Acquisition and Processing of Single-Cell RNA Sequencing Data

We obtained the HCC single-cell RNA sequencing dataset GSE202642, comprising seven tumor samples and four normal liver samples, from the GEO database (https://www.ncbi.nlm.nih.gov/geo/). Data preprocessing was performed using Seurat (v4.3.0) following three stringent quality control criteria: (1) cells with >25% mitochondrial gene content were excluded to remove stressed or dying cells; (2) cells with fewer than 200 or more than 8,000 detected genes were removed to avoid empty droplets and potential doublets; and (3) genes expressed in fewer than three cells were filtered out to eliminate low-information features. Normalization was performed using the NormalizeData function (log-normalization method, scale factor = 10,000), followed by identification of 2,000 highly variable genes (HVGs) with the FindVariableFeatures function (selection.method = "vst") to capture the most informative features for downstream analysis. The ScaleData function was applied to center and scale the data across all cells. Principal component analysis (PCA) was conducted to reduce dimensionality, and the first 30 principal components were used for batch effect correction via the Harmony (v0.1.1) algorithm (theta = 2, max.iter.harmony = 10), ensuring integration of data across different samples. Uniform manifold approximation and projection (UMAP) was performed with RunUMAP (dims = 1:20, min.dist = 0.1) for two-dimensional visualization, and clustering was carried out using FindNeighbors and FindClusters with a resolution parameter of 0.3 to identify distinct cellular subpopulations. Differentially expressed

genes (DEGs) for each cluster were identified using the FindAllMarkers function (Wilcoxon rank-sum test) with thresholds of adjusted p-value <0.05, |log2 fold change| >1, and expression ratio >0.1, ensuring the selection of robust cluster-specific markers. Cell type annotation was performed through dual validation by cross-referencing with the CellMarker database (v2023) and previously reported differential expression profiles,[30,31] thereby improving annotation accuracy. Visualization of cell distribution, marker expression, and QC metrics was achieved using the VlnPlot and FeatureScatter functions.

Acquisition and Processing of Transcriptomic and Gene Expression Data

HCC transcriptomic data from TCGA (https://portal.gdc.cancer.gov/) were log2-transformed. Single-sample gene set enrichment analysis (ssGSEA) was employed to quantify cellular NETs risk scores in the TCGA cohort.[32] External validation cohorts (GSE16757 and GSE104580) were included to ensure generalizability. We selected the two external datasets, GSE16757 and GSE104580, for validation primarily because they include survival follow-up data and have moderate sample sizes, enabling them to provide independent validation evidence separate from the TCGA cohort.

Quantification of NETs Signature Genes

NETs-related genes were curated from literature and the Molecular Signatures Database (MSigDB, https://www.gsea-msigdb.org/gsea/msigdb/).[33,34] MSigDB gene sets were retrieved using msigdbr (v7.5.1). 69 NETosis-associated genes were integrated (Supplementary Table 1). The PercentageFeatureSet function was used to quantify NETs signature activity at single-cell resolution. Cells were stratified into high/low expression subgroups based on median expression levels, and differentially expressed genes were identified using FindMarkers.

Identification of NETs-Related Genes

Weighted Gene Co-expression Network Analysis (WGCNA, v1.72-1) was applied to single-cell datasets to identify NETs score-associated gene modules.[35] This method constructs co-expression networks by calculating gene-gene correlation coefficients with weighted thresholds. Modules are defined based on gene expression patterns to detect gene clusters with high covariance. By correlating these gene clusters with phenotypic traits, the approach facilitates the discovery of potential biomarkers and therapeutic targets, providing critical insights for related studies.

Construction of a NETs-Related Prognostic Model

LASSO-COX regression analysis was performed on WGCNA-identified module genes to screen differentially expressed prognosis-related genes (DEPRGs) with $P<0.05$. Penalty parameters were optimized through 10-fold cross-validation (minimum partial deviation λ). Two optimal genes were selected, and their correlation coefficients were calculated. Risk scores were computed using a predefined formula, with Kaplan-Meier survival analysis conducted after stratifying patients into high/low-risk subgroups based on median scores.

Nomogram Development

A nomogram integrating risk stratification, and clinical factors (tumor stage, age, gender) was developed. Time-dependent ROC curves (AUC values), calibration curves, and decision curve analysis (DCA) were used to evaluate the model's clinical utility for 1/3/5-year survival prediction.

Enrichment Analysis

Differentially expressed genes (DEGs) between high- and low-risk groups in TCGA were identified using thresholds of $|FC|\geq1.5$ and $P<0.05$. Gene set enrichment analysis (GSEA) was performed to elucidate the biological functions of these DEGs.

Somatic Mutation Analysis

TCGA somatic mutation data were processed using the maftools package (v2.18.0). Waterfall plots were generated to visualize the distribution of high-frequency mutated genes and variant types.

Immune Infiltration Analysis and Drug Sensitivity Prediction

The ESTIMATE (v1.0.13) algorithm was used to calculate immune, stromal, and ESTIMATE scores between high-risk and low-risk HCC groups, with bubble plots visualizing intergroup differences. Tumor Immune Dysfunction and Exclusion (TIDE) algorithm predicted responses to immune checkpoint blockade therapy. Boxplots compared expression levels of immune checkpoint-related genes between subgroups.

Cell Culture and Transfection

HepG2 and Huh7 cells were purchased from the National Institute of Biological Products (Beijing, China) and cultured at 37 °C and 5% CO_2 in DMEM supplemented with 10% fetal bovine serum (Gibco) and 1% penicillin/streptomycin (Gibco). To investigate the function of the GAS2L3 gene, two specific siRNAs targeting GAS2L3 (GAS2L3-human-322, 5′ GCAUGAAGAGCUACAUGAATT3′; GAS2L3-human-843, 5'CCAAGCUCAAGUCUUCAAATT3') and a non-targeting control siRNA (NC) were designed and synthesized. Transfection of siRNAs into HepG2 and Huh7 cells was performed using Lipofectamine 3000 (Invitrogen) reagent. Cells were harvested for subsequent experiments 48 hours post-transfection.

Western Blot

Cells were lysed in RIPA-150 buffer containing protease inhibitor cocktail (Sigma). A total of 40 μg of protein was separated using SDS-PAGE and transferred to nitrocellulose membranes (Pall). The primary antibodies used were anti-GAPDH (10494-1-AP, Proteintech) and anti-GAS2L3 (25409-1-AP, Proteintech) overnight, followed by incubation with a secondary antibody.

EdU Proliferation Assay

To assess the effect of GAS2L3 on cell proliferation, an EdU assay was conducted. Transfected HepG2 and Huh7 cells were seeded into 96-well plates, and EdU reagent was added to each well. After 24 hours of incubation, the procedure was performed according to the EdU detection kit instructions (BeyoClick^{TM} EdU Cell Proliferation Kit with AF555, C0075S). The proportion of EdU-positive cells was analyzed by flow cytometry to evaluate cell proliferation capacity.

CCK-8 Cell Proliferation Assay

Seed cells in 96-well plates at a density of 1×10^3 cells per well. Add 10 μL CCK-8 to each well and incubate at 37°C for 12, 24, 36, and 48 hours. Cell proliferation is determined by measuring absorbance at 450 nm.

Statistical Analysis

Statistical analysis in this study was performed using R4.3.1. The experimental data were processed using GraphPad Prism 8.0. We performed three biological replicates for both the EdU and CCK-8 assays according to the experimental design. Normally distributed continuous variables were compared using *t*-test, while non-normally distributed variables were analyzed with Mann–Whitney *U*-test. Categorical variables were compared using χ^2 or Fisher's exact tests. Survival differences were assessed by Kaplan-Meier analysis with Log rank test. Spearman's rank correlation was used for association analysis, with $P<0.05$ considered statistically significant.

Results

Single-Cell RNA-Seq Data Processing and Cell Type Identification

Following quality control, single-cell RNA sequencing data were integrated using the RunHarmony algorithm to mitigate batch effects. Normalized data were log-transformed and subjected to dimensionality reduction via PCA and UMAP, enabling visualization of transcriptional heterogeneity. The FindClusters function partitioned cells into 21 transcriptomic clusters, ultimately identifying 11 distinct cell types: T cells, NK cells, macrophages, endothelial cells, epithelial cells, neutrophils, dendritic cells, B cells, monocytes, fibroblasts, and plasma cells (Figure 1A and B). Using the median NETs

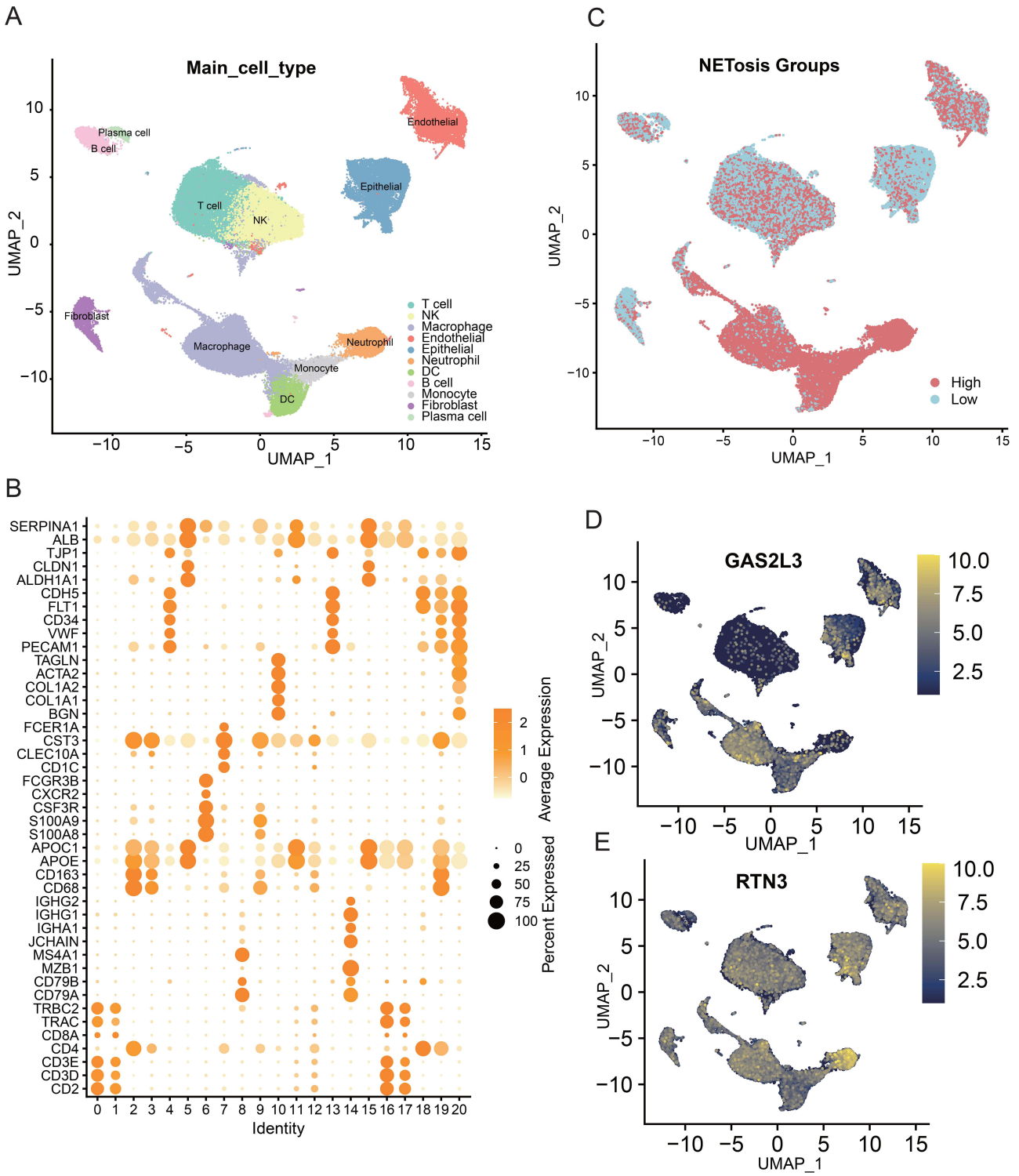

Figure 1 Single-cell RNA-Seq data processing and cell type identification. (**A** and **B**) Different cell types identified by the expression of surface marker genes. (**C**) Uniform manifold approximation and projection (UMAP) visualization of high- and low-NETs Subgroups. NETs: neutrophil extracellular traps. (**D**) Uniform manifold approximation and projection (UMAP) visualization of GAS2L3. (**E**) Uniform manifold approximation and projection (UMAP) visualization of RTN3.

score calculated via the PercentageFeatureSet method, all cells were stratified into high- and low-NETs subgroups, with their spatial distribution visualized on UMAP (Figure 1C). Differential gene analysis using the findmarker R package revealed GAS2L3 and RTN3 significantly dysregulated genes between high- and low-NETs subgroups (Figure 1D and E).

https://doi.org/10.2147/JHC.S546404

Identification of NETs -Related Gene Modules

WGCNA was performed on samples stratified by ssGSEA-derived NETs scores. With a soft thresholding power (β=4), deepSplit=2, and module merging threshold of 0.25, six co-expression modules were constructed (five non-gray modules and one gray module). Among these, the MEblue and MEyellow modules showed significant positive correlations with NETs scores, while the MEbrown module exhibited a significant negative correlation (Figure 2A–C). 288 candidate genes from these modules were selected for further investigation.

Prognostic Biomarker Screening and Validation

After screening candidate genes through LASSO regression (Figure 2D and E), the prognostic value of GAS2L3 and RTN3 was subsequently validated by multivariate Cox regression analysis, revealing that both GAS2L3 (HR=1.4, 95% *CI*: 1.1–1.7, *P*=0.001) and RTN3 (HR=1.7, 95% *CI*: 1.2–2.4, *P*=0.004) serve as independent prognostic factors (Figure 3A). In the TCGA cohort, the survival probability of patients with high expression levels of the GAS2L3 (HR=2.095, 95% *CI*: 1.469–2.988, $P < 0.0001$) and RTN3 (HR=2.05, 95% *CI*: 1.44–2.92, $P < 0.0001$) genes were significantly lower than those with low expression (Figure 3B). Based on the expression distribution of the two genes, GAS2L3 and RTN3, a risk score (high-risk and low-risk) and outcome (death and survival) status were established (Figure 3C). Kaplan-Meier analysis revealed significantly improved OS in the low-expression subgroups of both genes in the TCGA cohort (HR=2.208, 95% *CI*: 1.504–3.243, $P < 0.0001$) (Figure 3D) and the external validation dataset GSE16757 (HR=2.887, 95% *CI*: 1.5–5.56, $P = 0.00096$) (Figure 3E). To evaluate the generalizability of our prognostic model in advanced HCC, subgroup analysis of Tumor-Node-Metastasis (TNM) stage III–IV patients in the TCGA cohort (n = 85) confirmed its significant prognostic value via Kaplan–Meier analysis (HR=2.369, 95% *CI*: 1.278–4.392, $P = 0.017$) (Supplementary Figure 1). Additionally, significantly improved relapse-free survival (RFS) was observed in the low-expression subgroup within another external validation dataset, GSE16757 (HR=2.421, 95% *CI*: 1.276–4.594, $P = 0.00047$) (Figure 4A). ROC curves yielded 1-, 3-, and 5-year AUC values of 0.79, 0.69, and 0.65 in the TCGA cohort

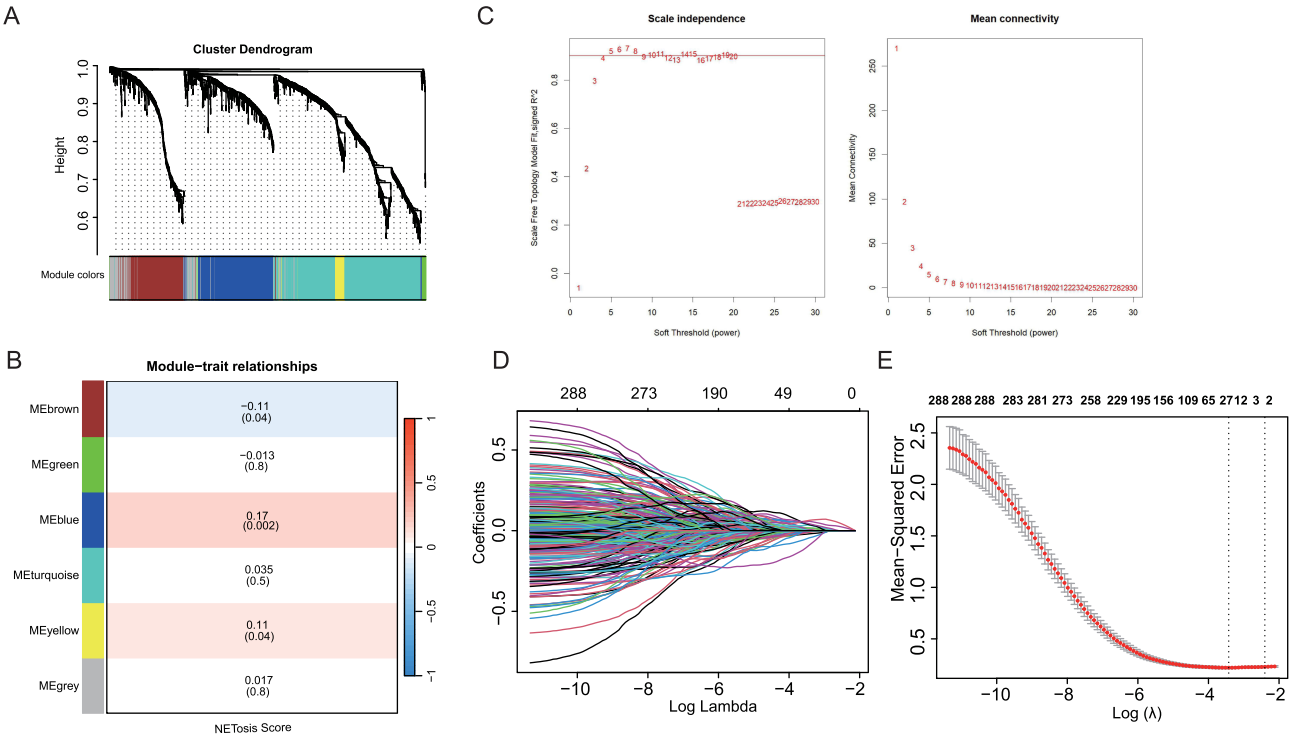

Figure 2 Identification of NETs-related gene modules and screening of differentially expressed genes. (**A**–**C**) Weighted Gene Co-expression Network Analysis (WGCNA) identifies NETs -related gene modules. (**D** and **E**) Candidate genes screening by LASSO regression.
Abbreviation: NETs, neutrophil extracellular traps.

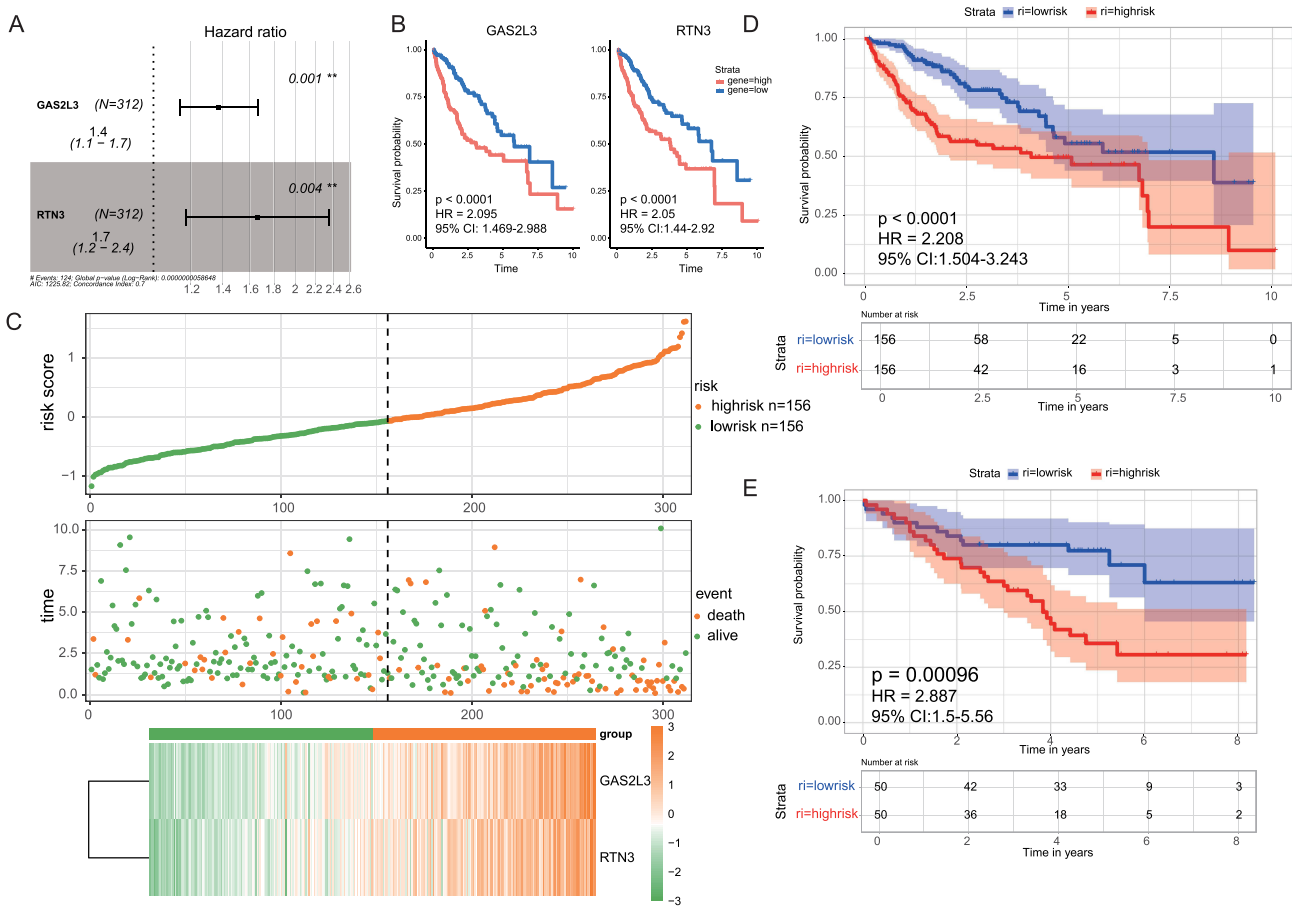

Figure 3 Prognostic value and clinical relevance of GAS2L3 and RTN3 in hepatocellular carcinoma. (**A**) Multivariate cox regression analysis validated the prognostic value of GAS2L3 and RTN3. (**B**) Kaplan-Meier survival curves showed the associations between GAS2L3/RTN3 expression levels and patient survival probability over time. (**C**) Risk score and outcome status based on GAS2L3 and RTN3 expression. (**D** and **E**) Kaplan-Meier analysis revealed significantly improved overall survival in the low-expression subgroups of both genes in the TCGA cohort (**D**) and the external validation dataset GSE16757 (**E**).

(Figure 4B), and 3-, 5-, and 8-year AUC values of 0.62, 0.73, and 0.64 in the external validation dataset GSE16757 (Figure 4C). In the TACE-treated cohort (GSE104580), responders exhibited significantly lower risk scores than non-responders (*P*=4.3e-09; Figure 4D).

Construction of a Prognostic Nomogram

To optimize HCC prognosis assessment, we developed a nomogram model integrating the NETs risk score with clinical parameters (Figure 5A). Within the prognostic signature model incorporating GAS2L3 and RTN3, patients in the high-expression subgroup exhibited significantly worse survival outcomes compared to those with low expression levels (HR=2.681, 95% *CI*: 1.804–3.985, $P < 0.0001$) (Figure 5B). In the TCGA cohort, the model demonstrated robust predictive performance for 1-, 3-, and 5-year OS, with AUC values of 0.734, 0.700, and 0.676, respectively (Figure 5C). DCA further confirmed the superior clinical utility of the nomogram in prognostic stratification and clinical decision-making compared to conventional clinical indicators (Figure 5D). Calibration curves revealed high concordance between predicted and observed survival outcomes, validating the model's accuracy (Figure 5E).

Enrichment Analysis

Significant disparities in the activation of immune-related pathways were observed between NETs risk subgroups (Figure 6A and B). In high-risk subgroups, the KEGG_GLYCOSPHINGOLIPID_BIOSYNTHESIS_LACTO_AND_NEOLACTO_ and KEGG_NEUROACTIVE_LIGAND_RECEPTOR_INTERACTION pathways exhibited pronounced enrichment,

https://doi.org/10.2147/JHC.S546404

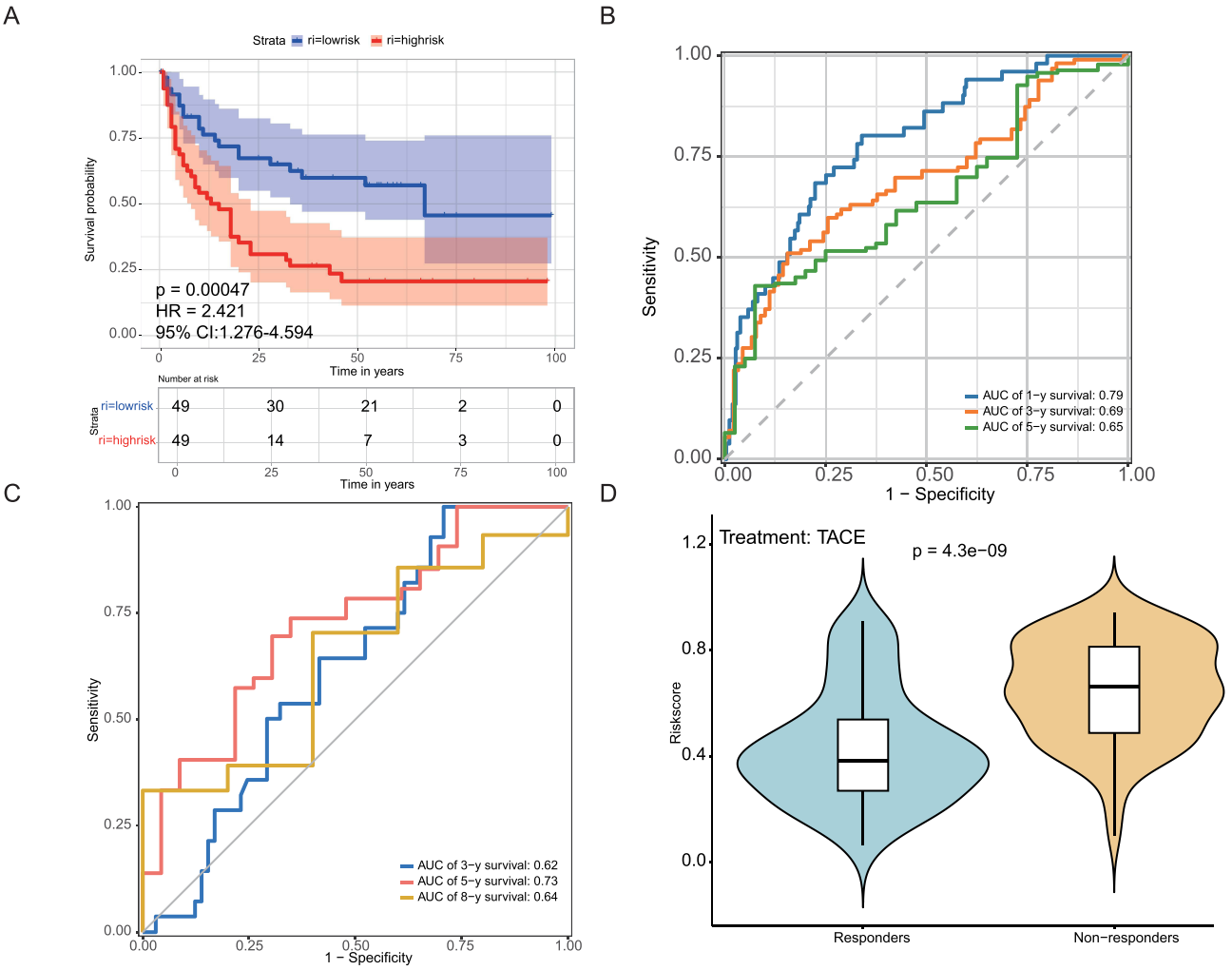

Figure 4 Prognostic impact and predictive accuracy of GAS2L3 and RTN3 expression in external validation cohorts. (**A**) Low expression of both genes correlated with enhanced relapse-free survival in the external validation dataset GSE16757. (**B**) Time-dependent ROC curves validated predictive accuracy in TCGA cohorts. (**C**) Time-dependent ROC curves validated predictive accuracy in GSE16757 cohorts. (**D**) Lower risk scores in responders compared to non-responders in the TACE-treated cohort (GSE104580).
Abbreviation: TACE, transcatheter arterial chemoembolization.

suggesting heightened glycosphingolipid biosynthesis activity that may promote tumor cell membrane remodeling, invasiveness, and neural infiltration within the tumor microenvironment (Figure 6A). These processes likely facilitate tumor growth and metastasis via neurotrophic factor secretion. Conversely, low-risk subgroups showed marked activation of the KEGG_LINOLEIC_ACID_METABOLISM pathway, indicative of synergistic anti-inflammatory, metabolic homeostatic, and immunomodulatory mechanisms (Figure 6B). This pathway activation may suppress chronic inflammation, maintain metabolic equilibrium, and optimize the immune microenvironment, thereby inhibiting tumor progression. The differential pathway activity patterns reflect distinct immune infiltration profiles between subgroups, which may underlie their divergent clinical outcomes.

Immune Infiltration and Mutational Landscape

The above analyses revealed significant differences in immune infiltration patterns and clinical outcomes between NETs-related risk subgroups. To further elucidate mechanisms underlying personalized immunotherapy, we compared mutational profiles and immune infiltration levels between high- and low-risk subgroups. High-risk subgroups exhibited higher overall mutation frequencies, with TP53, CTNNB1, and MUC16 being the most frequently mutated genes, predominantly via missense mutations (Figure 6C and D). Low-risk subgroups demonstrated elevated median Immune Scores, reflecting enhanced immune cell infiltration (P=0.011, Figure 7A). ESTIMATE Score (P=0.014; Figure 7B) and

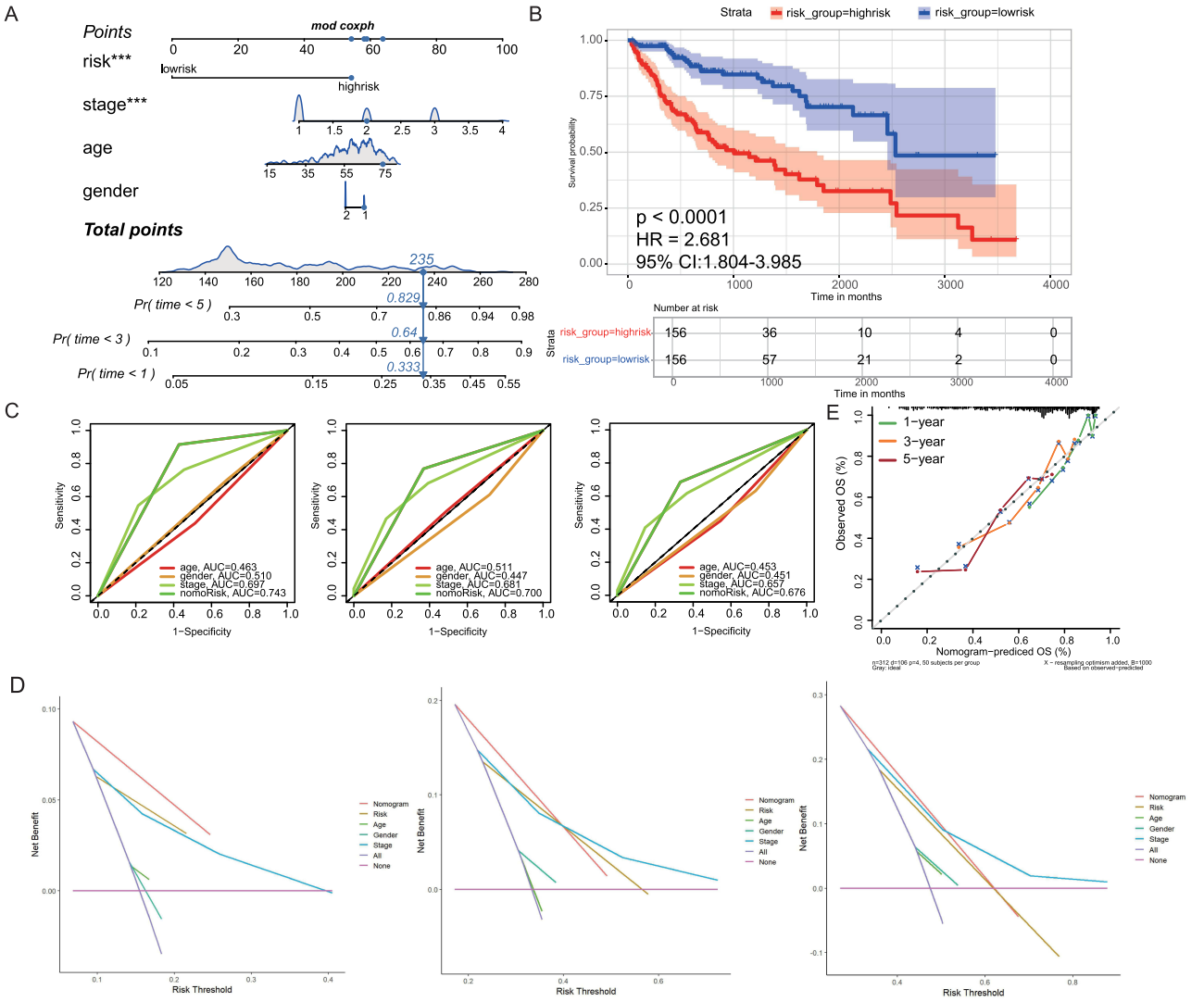

Figure 5 Development and validation of a nomogram model integrating NETs-related risk score with clinical parameters for prognosis prediction. (**A**) Development of a nomogram model combining the NETs risk score with clinical parameters. (**B**) High-expression subgroup in GAS2L3 and RTN3 prognostic signature model showed worse survival outcomes. (**C**) Time-dependent ROC curves validated the predictive accuracy of the model in the TCGA cohort (1-, 3-, and 5-Year overall survival Prediction). (**D**) Calibration curve showed high agreement between predicted and observed survival outcomes. (**E**) Decision curve analysis (DCA) confirmed superior clinical utility of the nomogram over traditional indicators.

Abbreviation: NETs, neutrophil extracellular traps.

Stromal Score (P=0.0057; Figure 7C) were significantly reduced in high-risk subgroups, indicating a tumor microenvironment characterized by stromal depletion and diminished immune infiltration. TIDE is an algorithm designed to predict the response of cancer patients to immune checkpoint inhibitors. It evaluates the potential for immune evasion by analyzing mechanisms of T cell dysfunction and exclusion within the tumor microenvironment, thereby predicting the likelihood of a patient's response to immunotherapy. A higher TIDE score indicates a greater risk of immune escape and a lower probability of benefiting from immunotherapy. Microsatellite Instability (MSI) refers to a characteristic of genomic instability in tumors. Tumors with high levels of MSI (MSI-H) generally exhibit greater immunogenicity and have a higher response rate to immune checkpoint inhibitor treatments. The MSI status can be determined through genetic testing and serves as one of the significant biomarkers for predicting the effectiveness of immunotherapy. Multidimensional evaluation using the TIDE algorithm revealed critical intergroup disparities: high-risk subgroups displayed elevated TIDE and Exclusion scores alongside reduced Dysfunction and MSI scores, suggesting concurrent enhancement of immune evasion and suppression of anti-tumor immune responses, indicative of dual inhibition of immune activity (Figure 7D).

https://doi.org/10.2147/JHC.S546404

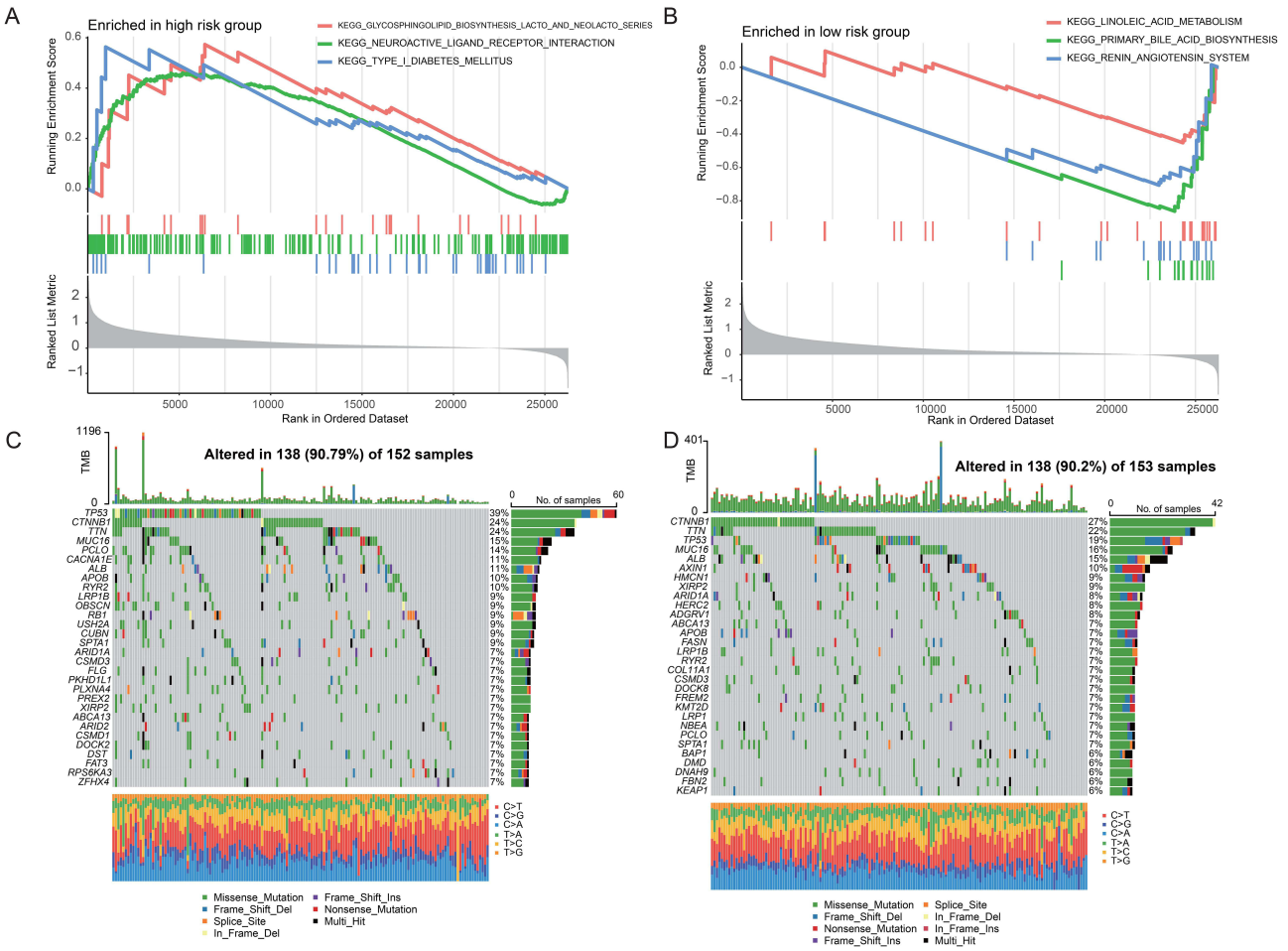

Figure 6 Comparison of immune-related pathways between NETs risk subgroups. (**A** and **B**) Significant differences in immune-related pathway activation between NETs risk subgroups. (**C** and **D**) Comparison of mutation profiles and immune infiltration levels between high- risk (**C**) and low-risk (**D**) subgroups.
Abbreviation: NETs: neutrophil extracellular traps.

Immune Checkpoint Expression Patterns

Building on the immune microenvironment heterogeneity identified by risk stratification, we further analyzed expression patterns of immune checkpoint-related genes (Figure 7E). Significant differential expression was observed between subgroups, particularly in TNFRSF18, TNFRSF4, VTCN1, HHLA2, and LAIR1. Low-risk subgroups exhibited upregulated expression of co-stimulatory molecules (TNFSF14) and immunoregulatory molecules (BTLA), whereas high-risk subgroups showed specific overexpression of immunosuppressive molecules (VTCN1, LAIR1). This expression heterogeneity aligns with previously observed therapeutic response disparities: the co-stimulatory signature in low-risk subgroups may enhance T-cell activation, while the immunosuppressive milieu in high-risk subgroups—driven by VTCN1-mediated T-cell exhaustion and LAIR1-dependent recruitment of myeloid-derived suppressor cells-collectively contributes to reduced sensitivity to immunotherapy.

GAS2L3 Knockdown Suppresses Proliferation of HepG2 and Huh7 Cells

Following knockdown of GAS2L3 using two distinct siRNAs, Western blot analysis revealed a significant reduction in GAS2L3 expression compared to NC, confirming efficient siRNA-mediated suppression of GAS2L3 (Figure 8A). Flow cytometry demonstrated markedly decreased proportions of EdU-positive cells in both siGAS2L3-1 and siGAS2L3-2 groups versus NC (Figure 8B left). Quantitative analysis of EdU-positive cells further validated significant reductions in proliferation for both siRNAs across HepG2 and Huh7 cells (Figure 8B right) ($P < 0.001$).

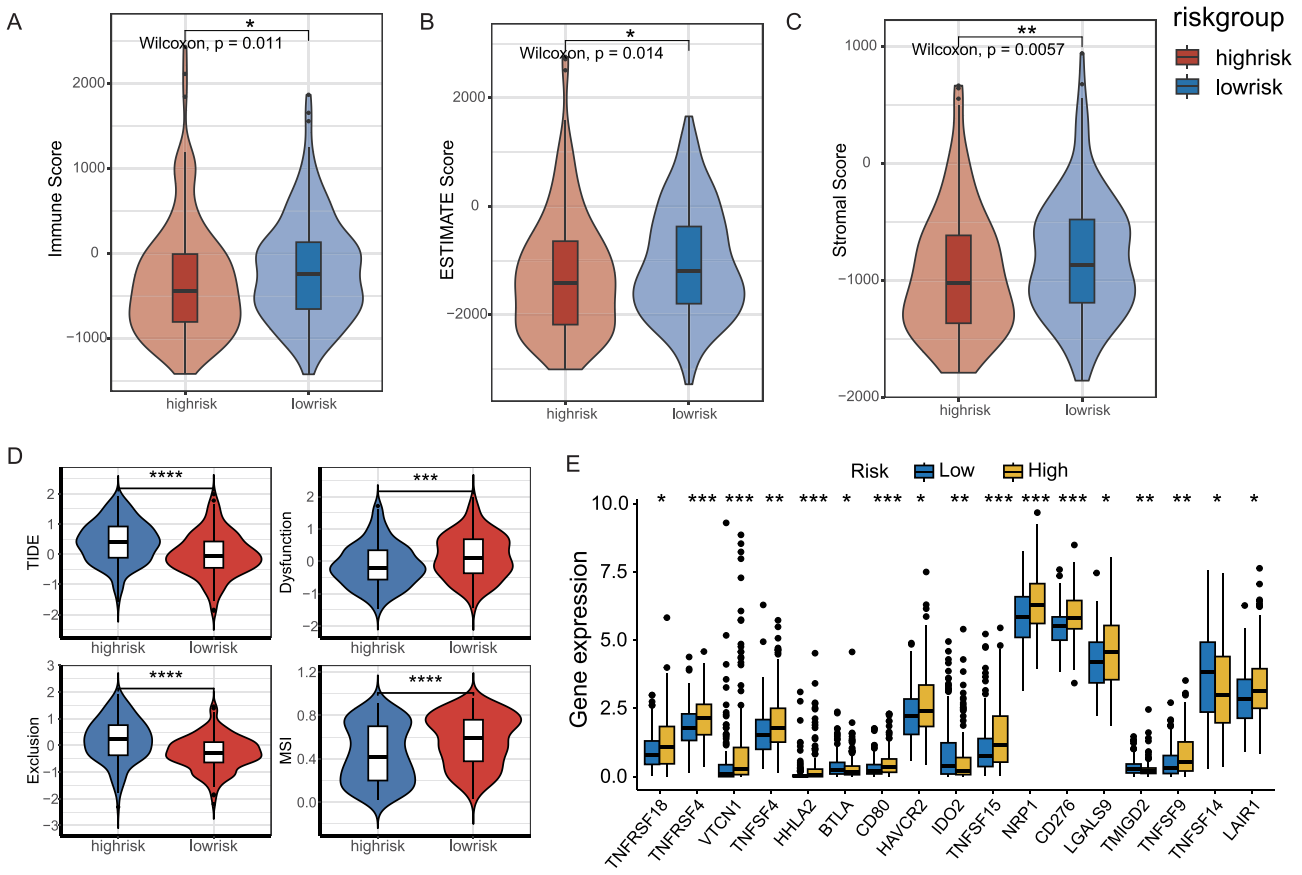

Figure 7 Comparison of immune infiltration and mutation landscape between NETs risk subgroups. (**A–C**) Comparison of immune scores (**A**), ESTIMATE scores (**B**) and stromal scores (**C**) between the high-risk and low-risk groups. (**D**) Comparison of Tumor Immune Dysfunction and Exclusion (TIDE), exclusion scores, dysfunction scores, and microsatellite instability (MSI) scores between the high-risk and low-risk groups. (**E**) Comparison of expression patterns of immune checkpoint-related genes between the high-risk and low-risk groups. *: $P < 0.05$; **: $P < 0.01$; ***: $P < 0.001$; ****: $P < 0.0001$.

CCK-8 assays evaluating the proliferative impact of GAS2L3 knockdown showed significantly lower OD450 values in siGAS2L3-treated HepG2 cells relative to NC, especially at 48 hours ($P < 0.001$; Figure 8C left). Consistent results were observed in Huh7 cells ($P < 0.01$; Figure 8C right). Collectively, these results establish that GAS2L3 knockdown inhibits proliferation in HCC lines HepG2 and Huh7.

Discussion

HCC, a highly malignant cancer with poor survival rates, represents a major global health burden.[36] Due to its complex etiology and pathogenesis, identifying key oncogenes involved in hepatocarcinogenesis is crucial. TME heterogeneity significantly contributes to the poor prognosis of HCC patients. Neutrophils, central players in the HCC immune landscape, regulate immunity, fight infections, and maintain tissue homeostasis. NETs have been strongly implicated in tumor growth, progression, and metastasis.[37] However, the role of NETosis-related genes in HCC immune defense remains poorly understood.[13]

Previous studies indicate that NETosis-targeting strategies for HCC can be classified into the following approaches. (1) Reducing NETs formation: Metformin lowers NETs levels and suppresses HCC metastasis.[38–40] (2) Inhibiting key NETosis enzymes: Sivelestat blocks neutrophil elastase, thereby reducing NETs formation and liver metastases in colorectal cancer models.[41] (3) Disrupting platelet-neutrophil interactions: Dual antiplatelet therapy (aspirin + ticagrelor) inhibits P-selectin-mediated aggregation and NETs release.[42,43] (4) Targeting mitochondrial dysfunction: In HCC, neutrophils produce pro-metastatic mtDNA-enriched NETs due to elevated mitochondrial ROS;[39] this can be mitigated by mesenchymal stromal cell-derived extracellular vesicles (MSC-EVs), which restore mitochondrial function,[44] while

https://doi.org/10.2147/JHC.S546404

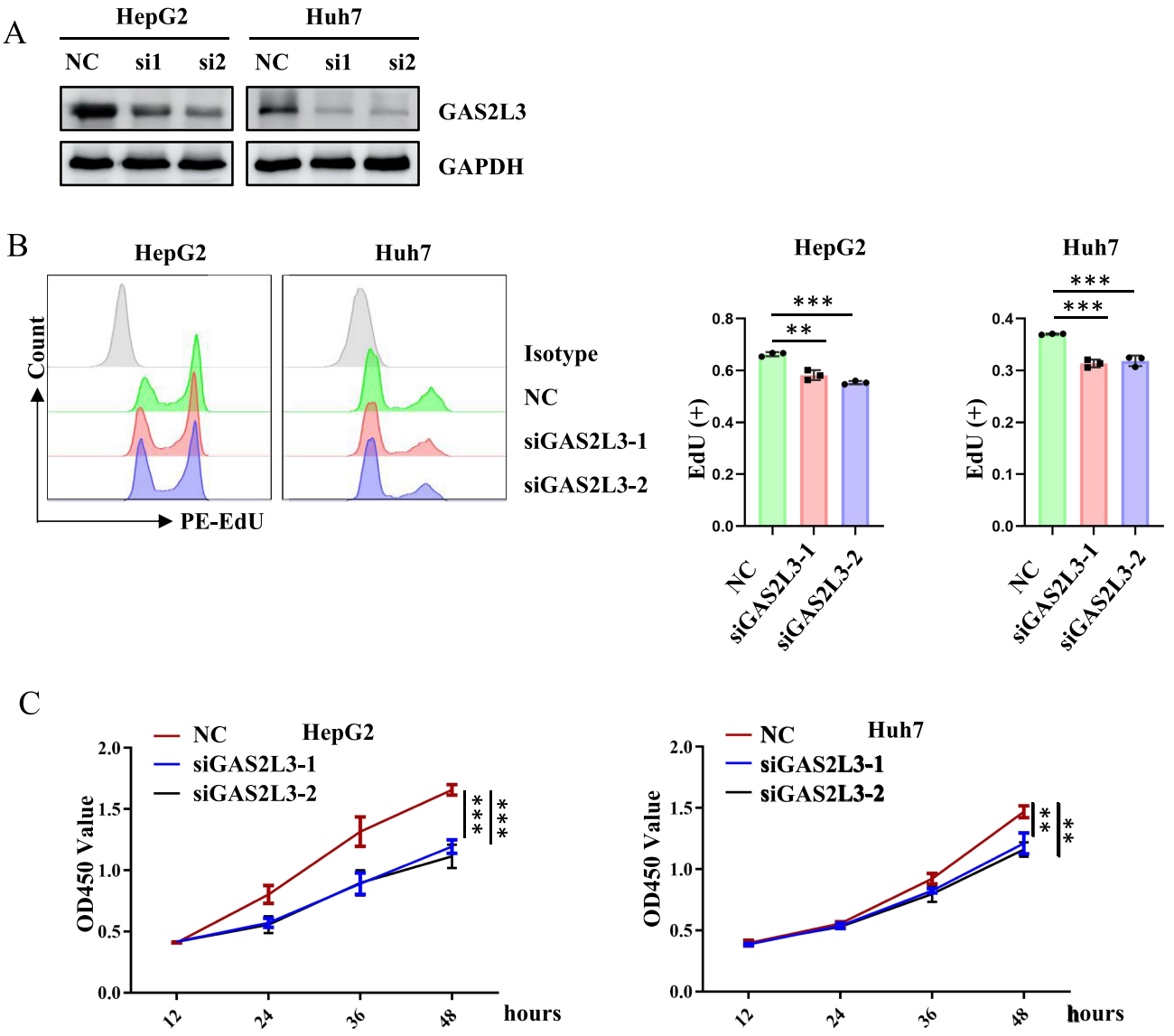

Figure 8 GAS2L3 knockdown suppressed proliferation of HepG2 and Huh7 cells. (**A**) Western blot confirmed effective siRNA-mediated suppression of GAS2L3. (**B**) Flow cytometry showed a significantly reduced proportion of EdU-positive cells in the siGAS2L3-1 and siGAS2L3-2 groups. (**C**) The CCK-8 cell proliferation assay demonstrated decreased OD450 values at 48 hours in siGAS2L3-treated HepG2 and Huh7 cells. **: $P < 0.01$; ***: $P < 0.001$.

metformin selectively impairs mitochondrial ATP synthesis in cancer cells.[19] (5) Degrading existing NETs: DNase I can degrade NETs components, but its short half-life limits clinical utility due to the need for frequent administration. To overcome this, an adeno-associated virus (AAV)-based gene therapy enables sustained, liver-targeted DNase I expression through a single injection, and its combination with anti-PD-1 therapy enhances CD8+ T cell infiltration and overcomes treatment resistance.[45] (6) Postoperative adjuvant therapy: A pH-responsive adhesive hemostatic hydrogel (GODM-gel), loaded with DNase I–containing mesoporous bioactive glass nanoparticles (MBGNs), neutralizes the acidic tumor microenvironment, degrades NETs, boosts NK cell infiltration, and prevents recurrence in orthotopic HCC models.[17]

Despite these promising therapeutic strategies, there remains a critical need for reliable gene signatures that can identify key drivers of NETosis and improve patient stratification in HCC. Gene signature models have been extensively employed in the prediction and diagnosis of various diseases. The strength of these models lies in their capacity to leverage high-throughput technologies for simultaneous detection of multiple gene expression levels, thereby capturing comprehensive molecular profiles and offering deeper insights into the biological mechanisms underlying diseases. In contrast, conventional clinical staging systems such as the TNM and Barcelona Clinic Liver Cancer (BCLC)

classifications, while widely used, have notable limitations. The TNM system, which stages tumors based on size (T), lymph node involvement (N), and distant metastasis (M), is a general oncological framework but poorly captures the biological heterogeneity of HCC, as it does not account for liver-specific factors such as cirrhosis or viral load.[46] The BCLC system improves upon this by incorporating tumor burden, liver function (Child-Pugh class), and performance status to guide treatment decisions; however, it remains limited in predicting recurrence risk in early-stage HCC and does not integrate molecular biomarkers.[47] Our study developed a robust NETs-related gene signature (GAS2L3 and RTN3) by integrating single-cell and bulk transcriptomic data from GSE202642 and TCGA, using WGCNA and LASSO-Cox regression to construct a prognostic risk model and nomogram for HCC. Comprehensive analyses revealed significant differences in biological functions, immune infiltration, and therapeutic vulnerabilities between risk groups, enhancing prognostic accuracy and identifying potential therapeutic targets. By embedding biological mechanism (NETs-mediated immunosuppression) into a predictive framework, our model complements and extends beyond traditional staging systems, offering a molecularly informed, mechanism-driven approach to risk stratification in HCC.

Members of the growth arrest-specific 2 (GAS2) protein family contain a putative actin-binding calponin homology (CH) domain and a microtubule-binding growth arrest–specific related (GAR) domain.[48] This protein family comprises four members: GAS2, GAS2-like protein 1 (GAS2L1), GAS2-like protein 2 (GAS2L2), and GAS2-like protein 3 (GAS2L3).[49] Notably, GAS2L3 is functionally implicated in mitotic regulation and cell division.[48] Emerging evidence highlights its critical role in tumor progression across multiple malignancies, including glioma[50,51] and esophageal squamous cell carcinoma.[52] Comparative analyses reveal significantly elevated GAS2L3 expression in HCC tissues compared to adjacent non-tumorous specimens.[53,54] Through pan-cancer profiling of GAS2 family members, Xu et al demonstrated that GAS2L3 exhibits elevated expression across diverse tumor types, functions as an independent prognostic factor in HCC patients, and correlates with immune cell infiltration, suggesting its potential oncogenic role in hepatocarcinogenesis.[53] Consistently, diethylnitrosamine (DEN)-induced HCC murine models recapitulate GAS2L3 upregulation in hepatic tumor tissues.[54] Furthermore, GAS2L3 has been incorporated into gene-based prognostic signatures for effectively predicting survival outcomes in HCC cohorts.[55] In our experimental framework, siRNA-mediated knockdown of GAS2L3 was successfully achieved in HepG2 and Huh7 hepatocellular carcinoma cell lines. Subsequent flow cytometry and quantitative analyses demonstrated that GAS2L3 suppression significantly inhibited cellular proliferation in both cell lines. Time-course experiments revealed progressively divergent growth patterns, with control groups exhibiting markedly higher OD450 values compared to GAS2L3-knockdown groups, particularly at the 48-hour time point. These findings collectively demonstrate that GAS2L3 depletion exerts potent anti-proliferative effects in HCC models.

Research has demonstrated that GAS2 plays a vital role in HCC cell proliferation and apoptosis, possibly by regulating the cell cycle and p53-dependent apoptosis pathway.[56] Elevated GAS2L3 expression shows promise for improving early HCC detection and risk stratification. Beyond its biomarker utility, elucidating the molecular mechanisms of GAS2L3 may unlock novel therapeutic strategies. Notably, investigating the potential role of GAS2L3 in NETosis could reveal novel therapeutic intervention points. Specifically, it is worth exploring whether GAS2L3 acts as an upstream regulator of key NETosis-associated enzymes—such as peptidylarginine deiminase 4 (PAD4), NE, and myeloperoxidase (MPO)—in response to inflammatory or hypoxic stimuli within the tumor microenvironment. If GAS2L3 promotes PAD4 activation or modulates NE and MPO activity through direct protein–protein interactions or post-translational modifications, targeting GAS2L3 may provide greater specificity than inhibiting downstream effectors, thereby reducing potential off-target effects on physiological immune functions. Furthermore, determining whether GAS2L3 integrates into the structural framework of NETs or influences their functional properties—such as stability, adhesiveness, or ability to trap tumor cells—through co-localization studies and functional assays would help define its biological significance. Validation of these mechanisms could elevate GAS2L3 from a prognostic biomarker to a therapeutically actionable target, paving the way for the development of small-molecule inhibitors, monoclonal antibodies, or gene-based therapies aimed at suppressing NETs-driven HCC metastasis. Future studies should validate these findings in larger patient cohorts, further investigate the biological functions of GAS2L3 in liver cancer, and evaluate the effectiveness of GAS2L3-directed treatments through clinical trials. Furthermore, the NETs-related gene signature may potentially be developed into a clinical molecular testing panel in the future, enabling risk stratification for patients after hepatocellular carcinoma surgery and aiding in the formulation of personalized follow-up strategies and immunotherapy

decisions. Moreover, since NETs themselves can be non-invasively detected through serum biomarkers (such as cfDNA and MPO-DNA complexes), this model holds strong potential for translation into a liquid biopsy-based application.

The endoplasmic reticulum protein Reticulon (RTN) family comprises four members: RTN1, RTN2, RTN3, and RTN4.[57] RTN3, an integral membrane protein, plays essential roles in endoplasmic reticulum morphogenesis and regulation of membrane-bound acyltransferase activity in normal cellular physiology.[58–60] Beyond its physiological functions, RTN3 has been implicated in Alzheimer's disease pathogenesis and astrocytoma progression. Although reported in HCC research, its functional role remains controversial. The study has shown that RTN3-mediated Chk2/p53 activation suppresses hepatocellular carcinogenesis and is inhibited by hepatitis B virus.[61] Other investigations demonstrate that RTN3 knockdown suppresses proliferation, migration, and invasion capabilities in HepG2 cells[62] while elevated RTN3 mRNA/protein levels in tumor tissues are positively correlated with unfavorable prognosis in multivariate risk models.[63] These conflicting observations suggest viral infection status may critically influence RTN3's functional duality in HCC. Our research data show that excessive RTN3 gene is associated with the proliferation, invasion, and metastasis of tumor cells.

In the high-risk NETs subgroup, activation of the KEGG_Glycosphingolipid_Biosynthesis_Lacto_and_Neolacto pathway was observed. This pathway refers to the specific biochemical processes involved in the biosynthesis of two distinct classes of glycosphingolipids (GSLs): the lacto-series and the neolacto-series. GSLs are amphipathic molecules composed of a lipid anchor (ceramide) and a glycan head group. As essential constituents of the plasma membrane, particularly within lipid rafts, they serve not only as structural elements but also as critical signaling molecules regulating diverse cellular processes, including cell adhesion, proliferation, differentiation, and apoptosis.[64] Regarding the lacto- and neolacto-series glycosphingolipids, accumulating evidence suggests their significant involvement in HCC. Notably, Zhu et al demonstrated that fucosylated glycosphingolipids are markedly overexpressed in HCC tumor tissues compared to adjacent non-tumorous liver tissues.[65] However, the precise functional roles and underlying mechanisms of fucosylated, as well as other lacto/neo-lacto series GSLs, in HCC progression and their potential as therapeutic targets or biomarkers remain incompletely understood. Further research is therefore warranted to elucidate the contribution of these specific glycosphingolipids to HCC pathogenesis and cancer biology more broadly.

This study has certain limitations. First, differences in sample sources, data preprocessing methods, and analytical techniques may lead to variations in gene signatures, thereby affecting the stability and reproducibility of prediction outcomes. While we have applied bioinformatics methods for batch correction, we cannot completely rule out the potential impact of residual batch effects or population heterogeneity on the model's generalizability. Although the current model demonstrates robust prognostic predictive performance across multiple public cohorts, we emphasize that its stability and clinical utility still require further validation in prospective, multicenter cohorts with standardized sampling protocols and uniform detection platforms. Additionally, the gene signature model is primarily constructed based on differences in gene expression levels, potentially neglecting other critical factors such as genetic variations and post-transcriptional modifications that could influence predictive performance. Therefore, when utilizing gene signature models, it is important to recognize their limitations and integrate additional biological information and experimental data to achieve a more comprehensive analysis. Finally, although the HepG2 cell line is widely used in hepatocellular carcinoma research, it is essential to note that this model may not fully recapitulate all aspects of the human condition.

Conclusion

To sum up, through the integration of multi-omics sequencing data, including single-cell RNA sequencing and transcriptomic profiles, we constructed a prognostic signature linked to NETs and thoroughly examined the clinical significance of high versus low NETs activity in hepatocellular carcinoma. Additionally, we identified GAS2L3 as a key NETs-associated gene, whose expression was strongly associated with tumor progression, highlighting its potential as a therapeutic target for HCC.

Data Sharing Statement

This study analyzed publicly available datasets. The data were derived from TCGA database, and the GSE202642, GSE16757 and GSE104580 in the GEO database, respectively. All data generated or analyzed during this study are available from the corresponding author upon reasonable request (Ronghua Jin, ronghuajin@ccmu.edu.cn).

Ethics Statement

We used data from publicly available databases. Studies included in the analysis were approved by relevant institutional review committees, and participants provided informed consent. The studies involving humans were approved by Ethics committee of Beijing You'an Hospital, Capital Medical University (LL-2022-080-K).

Acknowledgments

Ningning Lu and Zhixia Gu are co-first authors for this study. Thanks to TCGA and GEO databases and uploaders of the dataset.

Author Contributions

All authors made a significant contribution to the work reported, whether that is in the conception, study design, execution, acquisition of data, analysis and interpretation, or in all these areas; took part in drafting, revising or critically reviewing the article; gave final approval of the version to be published; have agreed on the journal to which the article has been submitted; and agree to be accountable for all aspects of the work.

Funding

This study received funding from Capital's Funds for Health Improvement and Research (2024-1-2171).

Disclosure

The authors declare no competing interests in this work.

References

1. Sung H, Ferlay J, Siegel RL. et al. Global Cancer Statistics 2020: GLOBOCAN Estimates of Incidence and Mortality Worldwide for 36 Cancers in 185 Countries. *CA Cancer J Clin*. 2021;71(3):209–249. doi:10.3322/caac.21660
2. Bray F, Laversanne M, Sung H, et al. Global cancer statistics 2022: GLOBOCAN estimates of incidence and mortality worldwide for 36 cancers in 185 countries. *CA Cancer J Clin*. 2024;74(3):229–263. doi:10.3322/caac.21834
3. Villanueva A. Hepatocellular Carcinoma. *N Engl J Med*. 2019;380(15):1450–1462. doi:10.1056/NEJMra1713263
4. Llovet JM, Pinyol R, Kelley RK, et al. Molecular pathogenesis and systemic therapies for hepatocellular carcinoma. *Nat Cancer*. 2022;3(4):386–401. doi:10.1038/s43018-022-00357-2
5. Lu Y, Yang A, Quan C, et al. A single-cell atlas of the multicellular ecosystem of primary and metastatic hepatocellular carcinoma. *Nat Commun*. 2022;13(1):4594. doi:10.1038/s41467-022-32283-3
6. Denk D, Greten FR. Inflammation: the incubator of the tumor microenvironment. *Trends Cancer*. 2022;8(11):901–914. doi:10.1016/j.trecan.2022.07.002
7. Waks Z, Weissbrod O, Carmeli B, Norel R, Utro F, Goldschmidt Y. Driver gene classification reveals a substantial overrepresentation of tumor suppressors among very large chromatin-regulating proteins. *Sci Rep*. 2016;6(1):38988. doi:10.1038/srep38988
8. Krajnović M, Kožik B, Božović A, Jovanović-Ćupić S. Multiple Roles of the RUNX Gene Family in Hepatocellular Carcinoma and Their Potential Clinical Implications. *Cells*. 2023;12(18):2303. doi:10.3390/cells12182303
9. Zheng J, Wang S, Xia L, et al. Hepatocellular carcinoma: signaling pathways and therapeutic advances. *Signal Transduct Target Ther*. 2025;10(1):35. doi:10.1038/s41392-024-02075-w
10. Rosales C. Neutrophils at the crossroads of innate and adaptive immunity. *J Leukoc Biol*. 2020;108(1):377–396. doi:10.1002/JLB.4MIR0220-574RR
11. Geh D, Leslie J, Rumney R, Reeves HL, Bird TG, Mann DA. Neutrophils as potential therapeutic targets in hepatocellular carcinoma. *Nat Rev Gastroenterol Hepatol*. 2022;19(4):257–273. doi:10.1038/s41575-021-00568-5
12. Cortez-Retamozo V, Etzrodt M, Newton A, et al. Origins of tumor-associated macrophages and neutrophils. *Proc Natl Acad Sci U S A*. 2012;109(7):2491–2496. doi:10.1073/pnas.1113744109
13. Yang Y, Yu S, Lv C, Tian Y. NETosis in tumour microenvironment of liver: from primary to metastatic hepatic carcinoma. *Ageing Res Rev*. 2024;97:102297. doi:10.1016/j.arr.2024.102297
14. Honda M, Kubes P. Neutrophils and neutrophil extracellular traps in the liver and gastrointestinal system. *Nat Rev Gastroenterol Hepatol*. 2018;15(4):206–221. doi:10.1038/nrgastro.2017.183
15. Brinkmann V, Reichard U, Goosmann C, et al. Neutrophil extracellular traps kill bacteria. *Science*. 2004;303(5663):1532–1535. doi:10.1126/science.1092385
16. Mutua V, Gershwin LJ. A Review of Neutrophil Extracellular Traps (NETs) in Disease: potential Anti-NETs Therapeutics. *Clin Rev Allergy Immunol*. 2021;61(2):194–211. doi:10.1007/s12016-020-08804-7
17. Cheng Y, Gong Y, Chen X, et al. Injectable adhesive hemostatic gel with tumor acidity neutralizer and neutrophil extracellular traps lyase for enhancing adoptive NK cell therapy prevents post-resection recurrence of hepatocellular carcinoma. *Biomaterials*. 2022;284:121506. doi:10.1016/j.biomaterials.2022.121506
18. Cools-Lartigue J, Spicer J, McDonald B, et al. Neutrophil extracellular traps sequester circulating tumor cells and promote metastasis. *J Clin Invest*. 2013;123(8):3446–3458. doi:10.1172/JCI67484
19. Yazdani HO, Roy E, Comerci AJ, et al. Neutrophil Extracellular Traps Drive Mitochondrial Homeostasis in Tumors to Augment Growth. *Cancer Res*. 2019;79(21):5626–5639. doi:10.1158/0008-5472.CAN-19-0800

20. Houghton AM, Rzymkiewicz DM, Ji H, et al. Neutrophil elastase-mediated degradation of IRS-1 accelerates lung tumor growth. *Nat Med*. 2010;16(2):219–223. doi:10.1038/nm.2084
21. Xiao Y, Cong M, Li J, et al. Cathepsin C promotes breast cancer lung metastasis by modulating neutrophil infiltration and neutrophil extracellular trap formation. *Cancer Cell*. 2021;39(3):423–437.e427. doi:10.1016/j.ccell.2020.12.012
22. Zhang Y, Song J, Zhang Y, et al. Emerging Role of Neutrophil Extracellular Traps in Gastrointestinal Tumors: a Narrative Review. *Int J Mol Sci*. 2022;24(1):334. doi:10.3390/ijms24010334
23. de Andrea CE, Ochoa MC, Villalba-Esparza M, et al. Heterogenous presence of neutrophil extracellular traps in human solid tumours is partially dependent on IL-8. *J Pathol*. 2021;255(2):190–201. doi:10.1002/path.5753
24. Kaltenmeier C, Yazdani HO, Morder K, Geller DA, Simmons RL, Tohme S. Neutrophil Extracellular Traps Promote T Cell Exhaustion in the Tumor Microenvironment. *Front Immunol*. 2021;12:785222. doi:10.3389/fimmu.2021.785222
25. Feng C, Li Y, Tai Y, et al. A neutrophil extracellular traps-related classification predicts prognosis and response to immunotherapy in colon cancer. *Sci Rep*. 2023;13(1):19297. doi:10.1038/s41598-023-45558-6
26. Zhao J, Xie X. Prediction of prognosis and immunotherapy response in breast cancer based on neutrophil extracellular traps-related classification. *Front Mol Biosci*. 2023;10:1165776. doi:10.3389/fmolb.2023.1165776
27. Zuo Y, Leng G, Leng P. Identification and validation of molecular subtype and prognostic signature for lung adenocarcinoma based on neutrophil extracellular traps. *Pathol Oncol Res*. 2023;29:1610899. doi:10.3389/pore.2023.1610899
28. Ji Z, Zhang C, Yuan J, et al. Predicting the immunity landscape and prognosis with an NCLs signature in liver hepatocellular carcinoma. *PLoS One*. 2024;19(4):e0298775. doi:10.1371/journal.pone.0298775
29. Wang L, Wang Q, Li Y, Qi X, Fan X. A signature based on neutrophil extracellular trap-related genes for the assessment of prognosis, immunoinfiltration, mutation and therapeutic response in hepatocellular carcinoma. *J Gene Med*. 2024;26(1):e3588. doi:10.1002/jgm.3588
30. Luecken MD, Theis FJ. Current best practices in single-cell RNA-seq analysis: a tutorial. *Mol Syst Biol*. 2019;15(6):e8746. doi:10.15252/msb.20188746
31. Satija R, Farrell JA, Gennert D, Schier AF, Regev A. Spatial reconstruction of single-cell gene expression data. *Nat Biotechnol*. 2015;33(5):495–502. doi:10.1038/nbt.3192
32. Aibar S, González-Blas CB, Moerman T, et al. SCENIC: single-cell regulatory network inference and clustering. *Nat Methods*. 2017;14(11):1083–1086. doi:10.1038/nmeth.4463
33. Zhang Y, Guo L, Dai Q, et al. A signature for pan-cancer prognosis based on neutrophil extracellular traps. *J Immunother Cancer*. 2022;10(6):e004210. doi:10.1136/jitc-2021-004210
34. Wu J, Zhang F, Zheng X, et al. Identification of renal ischemia reperfusion injury subtypes and predictive strategies for delayed graft function and graft survival based on neutrophil extracellular trap-related genes. *Front Immunol*. 2022;13:1047367. doi:10.3389/fimmu.2022.1047367
35. Langfelder P, Horvath S. WGCNA: an R package for weighted correlation network analysis. *BMC Bioinf*. 2008;9(1):559. doi:10.1186/1471-2105-9-559
36. Wang Y, Deng B. Hepatocellular carcinoma: molecular mechanism, targeted therapy, and biomarkers. *Cancer Metastasis Rev*. 2023;42(3):629–652. doi:10.1007/s10555-023-10084-4
37. Adrover JM, McDowell SAC, He XY, Quail DF, Egeblad M. NETworking with cancer: the bidirectional interplay between cancer and neutrophil extracellular traps. *Cancer Cell*. 2023;41(3):505–526. doi:10.1016/j.ccell.2023.02.001
38. Menegazzo L, Scattolini V, Cappellari R, et al. The antidiabetic drug metformin blunts NETosis in vitro and reduces circulating NETosis biomarkers in vivo. *Acta Diabetol*. 2018;55(6):593–601. doi:10.1007/s00592-018-1129-8
39. Yang LY, Shen XT, Sun HT, Zhu WW, Zhang JB, Lu L. Neutrophil extracellular traps in hepatocellular carcinoma are enriched in oxidized mitochondrial DNA which is highly pro-inflammatory and pro-metastatic. *J Cancer*. 2022;13(4):1261–1271. doi:10.7150/jca.64170
40. Wang G, Gao H, Dai S, et al. Metformin inhibits neutrophil extracellular traps-promoted pancreatic carcinogenesis in obese mice. *Cancer Lett*. 2023;562:216155. doi:10.1016/j.canlet.2023.216155
41. Okamoto M, Mizuno R, Kawada K, et al. Neutrophil Extracellular Traps Promote Metastases of Colorectal Cancers through Activation of ERK Signaling by Releasing Neutrophil Elastase. *Int J Mol Sci*. 2023;24(2):1118. doi:10.3390/ijms24021118
42. Etulain J, Martinod K, Wong SL, Cifuni SM, Schattner M, Wagner DD. P-selectin promotes neutrophil extracellular trap formation in mice. *Blood*. 2015;126(2):242–246. doi:10.1182/blood-2015-01-624023
43. Yoshimoto M, Kagawa S, Kajioka H, et al. Dual antiplatelet therapy inhibits neutrophil extracellular traps to reduce liver micrometastases of intrahepatic cholangiocarcinoma. *Cancer Lett*. 2023;567:216260. doi:10.1016/j.canlet.2023.216260
44. Lu T, Zhang J, Cai J, et al. Extracellular vesicles derived from mesenchymal stromal cells as nanotherapeutics for liver ischaemia-reperfusion injury by transferring mitochondria to modulate the formation of neutrophil extracellular traps. *Biomaterials*. 2022;284:121486. doi:10.1016/j.biomaterials.2022.121486
45. Xia Y, He J, Zhang H, et al. AAV-mediated gene transfer of DNase I in the liver of mice with colorectal cancer reduces liver metastasis and restores local innate and adaptive immune response. *Mol Oncol*. 2020;14(11):2920–2935. doi:10.1002/1878-0261.12787
46. Zhang T, Nie Y, Gu J, et al. Identification of Mitochondrial-Related Prognostic Biomarkers Associated With Primary Bile Acid Biosynthesis and Tumor Microenvironment of Hepatocellular Carcinoma. *Front Oncol*. 2021;11:587479. doi:10.3389/fonc.2021.587479
47. Trevisani F, Vitale A, Kudo M, et al. Merits and boundaries of the BCLC staging and treatment algorithm: learning from the past to improve the future with a novel proposal. *J Hepatol*. 2024;80(4):661–669. doi:10.1016/j.jhep.2024.01.010
48. Zhang N, Zhao C, Zhang X, et al. Growth arrest-specific 2 protein family: structure and function. *Cell Prolif*. 2021;54(1):e12934. doi:10.1111/cpr.12934
49. Chen T, Rohacek AM, Caporizzo M, et al. Cochlear supporting cells require GAS2 for cytoskeletal architecture and hearing. *Dev Cell*. 2021;56(10):1526–1540.e1527. doi:10.1016/j.devcel.2021.04.017
50. Zhou Y, Zhang L, Song S, et al. Elevated GAS2L3 Expression Correlates With Poor Prognosis in Patients With Glioma: a Study Based on Bioinformatics and Immunohistochemical Analysis. *Front Genet*. 2021;12:649270. doi:10.3389/fgene.2021.649270
51. Zhao C, Zhang N, Cui X, et al. Integrative analysis regarding the correlation between GAS2 family genes and human glioma prognosis. *Cancer Med*. 2021;10(8):2826–2839. doi:10.1002/cam4.3829
52. Yang J, Wu B, Li G, et al. Landscape of epithelial cell subpopulations in the human esophageal squamous cell carcinoma microenvironment. *Heliyon*. 2024;10(19):e38091. doi:10.1016/j.heliyon.2024.e38091
53. Xu YY, Bai RX, Zhang QR, Zhang S, Zhang JH, Du SY. A comprehensive analysis of GAS2 family members identifies that GAS2L1 is a novel biomarker and promotes the proliferation of hepatocellular carcinoma. *Discov Oncol*. 2024;15(1):220. doi:10.1007/s12672-024-01083-0

54. Gao X, Zhao C, Zhang N, et al. Genetic expression and mutational profile analysis in different pathologic stages of hepatocellular carcinoma patients. *BMC Cancer*. 2021;21(1):786. doi:10.1186/s12885-021-08442-y
55. Shi L, Shang X, Nie K, et al. Identification of potential crucial genes associated with the pathogenesis and prognosis of liver hepatocellular carcinoma. *J Clin Pathol*. 2021;74(8):504–512. doi:10.1136/jclinpath-2020-206979
56. Zhu RX, Cheng ASL, Chan HLY, Yang DY, Seto WK. Growth arrest-specific gene 2 suppresses hepatocarcinogenesis by intervention of cell cycle and p53-dependent apoptosis. *World J Gastroenterol*. 2019;25(32):4715–4726. doi:10.3748/wjg.v25.i32.4715
57. Yan R, Shi Q, Hu X, Zhou X. Reticulon proteins: emerging players in neurodegenerative diseases. *Cell Mol Life Sci*. 2006;63(7–8):877–889. doi:10.1007/s00018-005-5338-2
58. Zhu L, Xiang R, Dong W, Liu Y, Qi Y. Anti-apoptotic activity of Bcl-2 is enhanced by its interaction with RTN3. *Cell Biol Int*. 2007;31 (8):825–830. doi:10.1016/j.cellbi.2007.01.032
59. Lee JT, Lee TJ, Kim CH, Ns K, Kwon TK. Over-expression of Reticulon 3 (RTN3) enhances TRAIL-mediated apoptosis via up-regulation of death receptor 5 (DR5) and down-regulation of c-FLIP. *Cancer Lett*. 2009;279(2):185–192. doi:10.1016/j.canlet.2009.01.035
60. Chen Y, Zhao S, Xiang R. RTN3 and RTN4: candidate modulators in vascular cell apoptosis and atherosclerosis. *J Cell Biochem*. 2010;111 (4):797–800. doi:10.1002/jcb.22838
61. Song S, Shi Y, Wu W, et al. Reticulon 3-mediated Chk2/p53 activation suppresses hepatocellular carcinogenesis and is blocked by hepatitis B virus. *Gut*. 2021;70(11):2159–2171. doi:10.1136/gutjnl-2020-321386
62. Gong Q, Chen X, Liu F, Cao Y. Machine learning-based integration develops a neutrophil-derived signature for improving outcomes in hepatocellular carcinoma. *Front Immunol*. 2023;14:1216585. doi:10.3389/fimmu.2023.1216585
63. Li B, Feng W, Luo O, et al. Development and Validation of a Three-gene Prognostic Signature for Patients with Hepatocellular Carcinoma. *Sci Rep*. 2017;7(1):5517. doi:10.1038/s41598-017-04811-5
64. Byrne FL, Olzomer EM, Lolies N, Hoehn KL, Wegner MS. Update on Glycosphingolipids Abundance in Hepatocellular Carcinoma. *Int J Mol Sci*. 2022;23(9):4477. doi:10.3390/ijms23094477
65. Zhu J, Wang Y, Yu Y, et al. Aberrant fucosylation of glycosphingolipids in human hepatocellular carcinoma tissues. *Liver Int*. 2014;34(1):147–160. doi:10.1111/liv.12265